ELectronics EXpress

LETTER

IEICE Electronics Express, Vol.12, No.4, 1–12

A novel four-wing strange attractor born in bistability

Chunbiao Li[1], Ihsan Pehlivan[2], Julien Clinton Sprott[3], and Akif Akgul[2a)]

[1] *School of Electronic and Information Engineering, Nanjing University of Information Science and Technology, Nanjing 210044, China*

[2] *Department of Electric and Electronic Engineering, University of Sakarya, Sakarya, Turkey*

[3] *Department of Physics, University of Wisconsin-Madison, Madison, USA*

a) *aakgul@sakarya.edu.tr*

Abstract: Attractor merging can exist in chaotic systems with some kind of symmetry, which makes it possible to form a four-wing attractor from a bistable system. A relatively simple such case is described, which has robust chaos varying from a pair of coexisting symmetric single-wing attractors to a double-wing butterfly attractor, and finally to a four-wing attractor. Basic dynamical characteristics of the system are demonstrated in terms of equilibria, Jacobian matrices, Lyapunov exponents, and Poincaré sections. From a broad exploration of the dynamical regions, we observe robust chaos with embedded Arnold tongues of periodicity in selected parameter regions. The chaotic system with a wing structure has four nonlinear quadratic terms, one of the coefficients of which is a hidden isolated amplitude parameter, by which one can control the amplitude of two of the variables. The corresponding chaotic circuit with an amplitude-control knob is designed and implemented, which generates a four-wing attractor with adjustable amplitude.

Keywords: four-wing attractor, bistability, hidden amplitude parameter

Classification: Electron devices, circuits, and systems

References

[1] M. E. Yalcin, J. A. K. Suykens, J. Vandewalle and S. Ozoguz: Int. J. Bifurcat. Chaos **12** (2002) 23. DOI:10.1142/S0218127402004164

[2] J. Lu, G. Chen and X. Yu: IEEE Trans. Circuits Syst. I, Fundam. Theory Appl. **51** (2004) 2476. DOI:10.1109/TCSI.2004.838151

[3] C. Li, I. Pehlivan and J. C. Sprott: Turkish J. Electr. Eng. Comput. Sci. DOI:10.3906/elk-1301-55

[4] E. Dong, Z. Chen, Z. Chen and Z. Yuan: Chin. Phys. B **18** (2009) 2680. DOI:10.1088/1674-1056/18/7/010

[5] G. Qi, G. Chen, S. Li and Y. Zhang: Int. J. Bifurcat. Chaos **16** (2006) 859. DOI:10.1142/S0218127406015180

[6] I. Pehlivan: OAM-RC **5** (2011) 1003.

[7] G. Qi, G. Chen, M. A. Van Wyk, B. J. Van Wyk and Y. Zhang: Chaos Solitons Fractals **38** (2008) 705. DOI:10.1016/j.chaos.2007.01.029

[8] S. Cang, G. Qi and Z. Chen: Nonlinear Dyn. **59** (2010) 515. DOI:10.1007/

DOI: 10.1587/elex.12.20141116
Received November 27, 2014
Accepted January 20, 2015
Publicized February 3, 2015
Copyedited February 25, 2015

s11071-009-9558-0
[9] S. Yu and G. Chen: IEEE Trans. Circuits Syst. II, Exp. Briefs **57** (2010) 803. DOI:10.1109/TCSII.2010.2067792
[10] S. Yu, G. Chen and X. Yu: IEEE Trans. Circuits Syst. II, Exp. Briefs **58** (2011) 314. DOI:10.1109/TCSII.2011.2149090
[11] S. Yu, X. Yu and G. Chen: IEEE Trans. Circuits Syst. I, Fundam. Theory Appl. **59** (2012) 1015. DOI:10.1109/TCSI.2011.2180429
[12] C. Li and J. C. Sprott: Phys. Lett. A **378** (2014) 178. DOI:10.1016/j.physleta.2013.11.004
[13] J. C. Sprott, X. Wang and G. Chen: Int. J. Bifurcat. Chaos **23** (2013) 1350093. DOI:10.1142/S0218127413500934
[14] C. Li and J. C. Sprott: Int. J. Bifurcat. Chaos **24** (2014) 1450034. DOI:10.1142/S0218127414500345
[15] C. Li and J. C. Sprott: Int. J. Bifurcat. Chaos **23** (2013) 1350199. DOI:10.1142/S021812741350199X
[16] C. Li, J. C. Sprott and W. Thio: J. Exp. Theor. Phys. **118** (2014) 494. DOI:10.1134/S1063776114030121
[17] C. Li and D. Wang: Acta Phys. Sin. **58** (2009) 764. DOI:10.7498/aps.58.764
[18] C. Li, H. Wang and S. Chen: Acta Phys. Sin. **59** (2010) 783. DOI:10.7498/aps.59.778
[19] C. Li, J. Wang and W. Hu: Nonlinear Dyn. **68** (2012) 575. DOI:10.1007/s11071-011-0239-4
[20] O. E. Sommerer, J. C. Alexander, I. J. C. Kan and J. A. Yorke: Physica D **76** (1994) 384. DOI:10.1016/0167-2789(94)90047-7
[21] C. Li and J. C. Sprott: Nonlinear Dyn. **73** (2013) 1335. DOI:10.1007/s11071-013-0866-z

1 Introduction

The study of chaotic behavior in nonlinear systems has attracted considerable attention due to the many possible applications in various fields of science and technology. Much research has been devoted to searching for new chaotic systems of autonomous ordinary differential equations (ODEs) with particular desired dynamic properties. With improvements in circuit realization technology through the development of integrated circuits, multi-scroll [1, 2, 3] and multi-wing chaotic systems have aroused special interest, especially four-wing attractors [4, 5, 6, 7, 8] and grid multi-wing chaotic systems [9, 10, 11]. It is known that wing attractors from a chaotic system generally arise from some symmetry, and when that symmetry is broken, the chaotic flow may drop into a different petal of the wing. The study of wing-structure attractors could possibly be used in pattern identification and contribute to the knowledge of structure dynamics. Many four-wing chaotic systems have three quadratic terms. However, additional nonlinear terms can make the chaotic attractor more elegant and have a higher dimension. In this paper, we introduce a new chaotic system with four quadratic terms that displays an elegant four-wing fractal structure.

As in many systems with some kind of symmetry, it is relatively common to find multistability and coexisting attractors in some regions of parameter space [12, 13, 14, 15, 16]. However, the new system introduced here has some distinct

DOI: 10.1587/elex.12.20141116
Received November 27, 2014
Accepted January 20, 2015
Publicized February 3, 2015
Copyedited February 25, 2015

features: (1) It generates a four-wing chaotic attractor with fractal structure for some choices of the parameters. (2) In a selected parameter region, it displays robust chaos with periodic Arnold tongues, and the strange attractor varies among a symmetric pair of single-wing attractors, a double-wing butterfly attractor, and a four-wing attractor. (3) There is a hidden parameter in the coefficient of a quadratic nonlinearity in the system, which is unlike chaotic systems with absolute value nonlinearities [17, 18, 19], whereby an obvious constant term controls the amplitude of all variables. For the circuit design of a chaotic system, a linear scaling of the variables is usually necessary to avoid saturation of the analog multipliers and operational amplifiers. In the new system, the coefficient of one quadratic term in the equation that contains a constant provides amplitude control of two of the variables without changing the Lyapunov exponent spectrum. Based on this property, an amplitude controllable circuit was designed and constructed.

In Sec. 2, we present the novel chaotic attractor with elegant four-wing structure from three first-order autonomous ODEs. Numerical results involving phase portraits, Lyapunov exponents, and Poincaré sections are presented. In Sec. 3, basic dynamical properties of the four-wing system are discussed including equilibria, Jacobian matrices, and symmetry characteristics. In Sec. 4, the dynamical region is explored in a selected parameter space, and the route from a single-wing attractor to the four-wing structure is shown along with the attractor basins. In Sec. 5, the hidden amplitude parameter is shown, and the corresponding amplitude-adjustable chaotic circuit is designed and implemented. The conclusions are summarized in Sec. 6.

2 Four-wing chaotic attractor

Based on existing research with four-wing chaotic systems, and with the motivation of including more cross-product terms and a constant term to generate a novel four-wing chaotic structure, the following set of three first-order, autonomous ODEs with four quadratic terms was considered:

$$\begin{cases} \dot{x} = ax + y + yz, \\ \dot{y} = -xz + yz, \\ \dot{z} = -z - mxy + b, \end{cases} \tag{1}$$

System (1) has four quadratic nonlinearities without any linear term in the second dimension of the equations, which makes it different from most other common systems. The four-wing chaotic attractor with $a = b = m = 1$ is displayed in various views in Fig. 1 for initial conditions of $(x_0, y_0, z_0) = (1, -1, 1)$. The attractor resembles two groups of butterfly shapes, which is different from other reported four-wing systems. Fig. 1 shows that the new four wings are built in different ways. Two of them are like auxiliary wings, and the other two are like master wings with the two groups extending in different directions.

Lyapunov exponents are the average exponential rates of divergence or convergence of state space trajectories. The Lyapunov exponents of the four-wing chaotic system (1) are found to be L1 = 0.409, L2 = 0, L3 = −1.773. The system has a relatively high Kaplan-Yorke dimension of $D_{KY} = 2.231$. Fig. 2 shows the

DOI: 10.1587/elex.12.20141116
Received November 27, 2014
Accepted January 20, 2015
Publicized February 3, 2015
Copyedited February 25, 2015

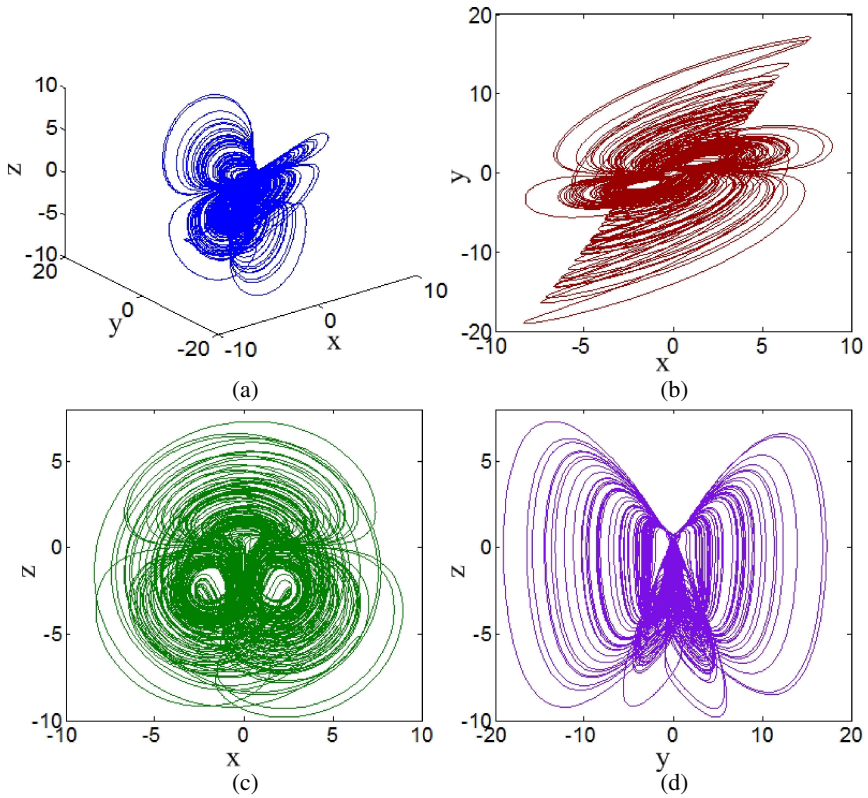

Fig. 1. Four-wing chaotic attractor, (a) 3-D view, (b) *x*-*y* plane, (c) *x*-*z* plane, (d) *y*-*z* plane.

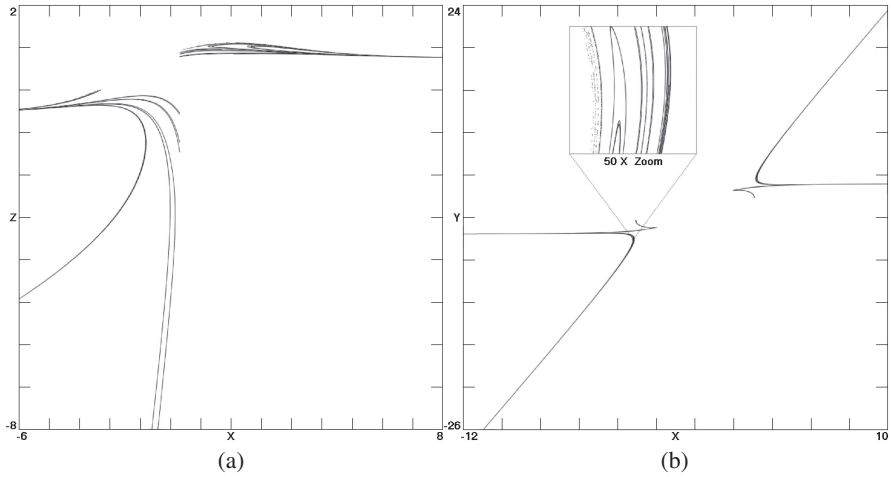

Fig. 2. Poincaré maps in planes where (a) $y = -0.7$, (b) $z = -3.0$

Poincaré sections in planes where $y = -0.7$ and $z = -3.0$, respectively. The Poincaré section in Fig. 2(b) contains four main branches and many twigs which show that it is a four-wing chaotic attractor with fractal structure.

3 Basic properties

3.1 Equilibria

The equilibria of the new four-wing system (1) can be found from

DOI: 10.1587/elex.12.20141116
Received November 27, 2014
Accepted January 20, 2015
Publicized February 3, 2015
Copyedited February 25, 2015

$$\begin{cases} \dot{x} = ax + y + yz = 0, \\ \dot{y} = -xz + yz = 0, \\ \dot{z} = -z - mxy + b = 0, \end{cases} \tag{2}$$

When m > 0, the system possesses five equilibrium points, i.e.,

$$\begin{aligned} P_1 &= (0, 0, b), \\ P_2 &= \left(-\tfrac{\sqrt{a+b+1}}{\sqrt{m}}, -\tfrac{\sqrt{a+b+1}}{\sqrt{m}}, -(a+1)\right), \\ P_3 &= \left(\tfrac{\sqrt{a+b+1}}{\sqrt{m}}, \tfrac{\sqrt{a+b+1}}{\sqrt{m}}, -(a+1)\right), \\ P_4 &= \left(-\tfrac{\sqrt{b}}{\sqrt{ma}}i, \tfrac{\sqrt{ab}}{\sqrt{m}}i, 0\right), \\ P_5 &= \left(\tfrac{\sqrt{b}}{\sqrt{ma}}i, \tfrac{-\sqrt{ab}}{\sqrt{m}}i, 0\right), \end{aligned} \tag{3}$$

For a, b, m positive, two of these points are imaginary, and three are real. These equilibria are symmetric about the z axis. When $a = b = m = 1$, the corresponding equilibrium points are $P_1 = (0, 0, 1)$, $P_2 = (-\sqrt{3}, -\sqrt{3}, -2)$, $P_3 = (\sqrt{3}, \sqrt{3}, -2)$, $P_4(-i, i, 0)$ and $P_5(i, -i, 0)$. An interesting feature is that the system has only three real equilibrium points, which is unusual and unexpected for a four-wing attractor.

3.2 Jacobian matrices

The Jacobian matrix of system (1) is given by

$$J = \begin{bmatrix} a & 1+z & y \\ -z & z & y-x \\ -my & -mx & -1 \end{bmatrix} \tag{4}$$

For $a = b = m = 1$, the Jacobian matrix at the first equilibrium P1 $= (0, 0, 1)$ is given by

$$J = \begin{bmatrix} 1 & 1+z & y \\ -z & z & y-x \\ -y & -x & -1 \end{bmatrix} = \begin{bmatrix} 1 & 2 & 0 \\ -1 & 1 & 0 \\ 0 & 0 & -1 \end{bmatrix} \tag{5}$$

From $|\lambda I - J_1| = 0$, the eigenvalues of the Jacobian matrix J_1 are $\lambda_1 = -1.0000$, $\lambda_2 = 1 + 1.4142i$, and $\lambda_3 = 1 - 1.4142i$. Here λ_1 is a negative real number, while λ_2 and λ_3 are a pair of complex conjugate eigenvalues with positive real parts. Consequently, the equilibrium P_1 is a saddle-focus, and the system (1) is unstable at the P_1 equilibrium point.

For the second equilibrium $P_2 = (-\sqrt{3}, -\sqrt{3}, -2)$, the eigenvalues are $\lambda_1 = -2.4082$, $\lambda_2 = 0.2041 + 2.2229i$, and $\lambda_3 = 0.2041 - 2.2229i$. For the third equilibrium $P_3 = (\sqrt{3}, \sqrt{3}, -2)$, the eigenvalues are identical to those of P_2. Consequently, all the real equilibrium points are saddle-foci, and the system (1) is unstable at those points. Also the eigenvalues of the Jacobian matrix at the imaginary equilibrium points were calculated. These eigenvalues are the same, $\lambda_1 = 1.5874$, $\lambda_2 = -0.7937 + 1.3747i$, and $\lambda_3 = -0.7937 - 1.3747i$ where λ_1 is a positive real number, and λ_2 and λ_3 are a pair of complex conjugate eigenvalues with negative real parts, which indicates that these two imaginary equilibrium points are saddle points.

DOI: 10.1587/elex.12.20141116
Received November 27, 2014
Accepted January 20, 2015
Publicized February 3, 2015
Copyedited February 25, 2015

3.3 Symmetry characteristics

System (1) is symmetric with respect to the z-axis, which can be easily shown by the coordinate transformation $(x, y, z) \rightarrow (-x, -y, z)$. Equilibrium points P_2, P_3, P_4, and P_5 are also symmetric with respect to the z-axis. The rotationally invariant chaotic system suggests that there is a hidden amplitude parameter m in the third dimension of the equation as will be shown later.

4 Robust chaos in a mixture of wing attractors with Arnold tongues

Since system (1) has eight terms, it has four bifurcation parameters with four of the coefficients set to unity by a linear rescaling of x, y, z, and t. To further explore the special dynamics of the system, we show in Fig. 3 the dynamical regions as determined from the Lyapunov exponent spectra in the space of the parameters a and b with $m = 1$. For this plot, initial conditions were chosen randomly from a Gaussian distribution of mean zero and variance one for each of the 800×800 pixels.

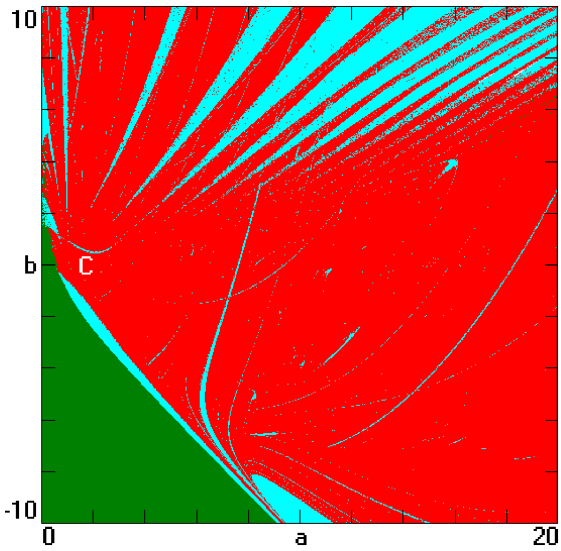

Fig. 3. Regions of various dynamical behaviors as a function of the bifurcation parameters a and b with $m = 1$. The chaotic regions are shown in red, the periodic regions are shown in blue, and the fixed-point regions are shown in green.

From the dynamical regions, we conclude the following:

(1) In the parameter space of $a[0, 20]$ and $b[-10, 10]$ with $m = 1$, the chaotic state is overwhelmingly dominant but with windows of periodicity, suggesting that the system has robust chaos in this parameter space.

(2) There are two special areas in the figure, a green triangular area in the lower-left corner representing point attractors and a cluster of blue bands of Arnold tongues in the upper-right representing limit cycles. For the first equilibrium point of the system, the characteristic equation is $\lambda^3 + (1 - a - b)\lambda^2 + (ab - a + b^2)\lambda + ab + b(b + 1) = 0$, while for the second and third equilibrium points, the characteristic equation is $\lambda^3 + 2\lambda^2 + (a + b + 2)\lambda + 2(a + b + 1)(a + 1) = 0$. Thus according to

DOI: 10.1587/elex.12.20141116
Received November 27, 2014
Accepted January 20, 2015
Publicized February 3, 2015
Copyedited February 25, 2015

the Routh-Hurwitz stability criterion, there is a boundary given by $a = 0.5(-b - 1 + \sqrt{(b+1)^2 + 4})$ that divides the plot into regions of unstable saddle-focus and stable focus. The limit cycles in different tongues have the attractors of a symmetric pair of limit cycles or one symmetric one, as shown in Fig. 4(a)–(b). Different types of limit cycles change alternately in different Arnold tongues.

(3) There is a slight blue gap between green and red, which suggests that the system has a typical bifurcation from point attractor to limit cycle to chaos in that region.

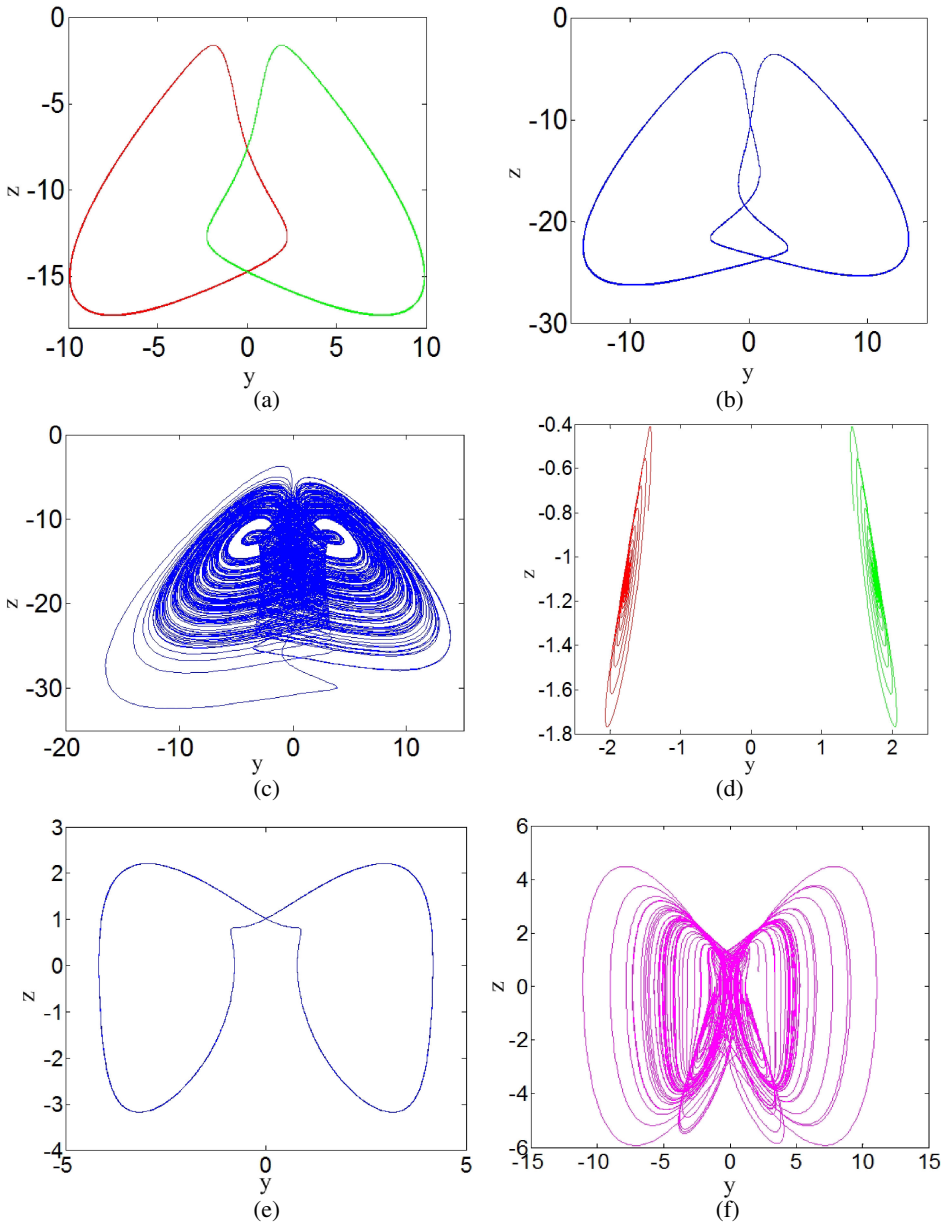

Fig. 4. Phase portrait in the y-z plane with $m = 1$ (red and green with symmetric initial conditions $(x_0, y_0, z_0) = \pm 1, \mp 1, 1$ (a) limit cycles in Arnold tongues ($a = 4.5$, $b = 8$) (b) limit cycles in Arnold tongues (a = 8, b = 8) (c) double-wing butterfly attractor ($a = 10$, $b = 0$) (d) point attractors ($a = 0.11$, $b = 2$) (e) symmetric limit cycle ($a = 0.12$, $b = 2$) (f) four-wing attractor ($a = 0.45$, $b = 2$).

DOI: 10.1587/elex.12.20141116
Received November 27, 2014
Accepted January 20, 2015
Publicized February 3, 2015
Copyedited February 25, 2015

(4) The system displays three routes to a wing attractor, each of which arises from a specific bistability. The first approach to a wing attractor is from coexisting point attractors to a strange attractor directly. In this case, the coexisting point attractors suddenly lose their stability, and the system evolves into a double-wing attractor. This phenomenon happens in those areas with immediate connection between green and red, typically $b = 0$. A robust double-wing butterfly attractor is generated by this method, as shown in Fig. 4(c).
(5) This route is indicated by a limit cycle bubble on the top of the green triangle with a typical value $b = 2$. Here a symmetric limit cycle is born from two coexisting point attractors and then suddenly bursts into a four-wing attractor, as shown in Fig. 4(d)–(f).
(6) The third route is indicated by another limit cycle bubble attached beside the top of the green triangle with a typical value $a = 11$. With an increasing b, the system displays bistability of limit cycles and a symmetric pair of single-wing strange attractors. The symmetric pair of single-wing attractors merge suddenly to a double-wing butterfly structure. With a further increase of b, the double-wing structure suddenly bursts into a four-wing attractor with the catalysis of limit cycles in Arnold tongues. The coexisting single-wing attractors and their attractor basins are shown in Fig. 5(a)–(b). In the cross-section of the fractal basins of attraction in the $x = 0$ plane, the black lines are cross sections of the corresponding strange attractors that almost touch their basin boundaries.
(7) The dotted area at the upper-right of Fig. 3 suggests that there is multistablity with different types of attractors. At large a and b the four-wing strange attractor and a symmetric pair of limit cycles share the basin of attraction, as shown in Fig. 6(a)–(b). In the cross-section of the fractal basins of attraction in the $x = 0$ plane, the black lines are cross sections of the corresponding four-wing strange attractors. Note that much of the plot contains regions where the three colors are closely intermingled suggesting the existence of riddled basins [20]. This behavior persists in a 30-times zoom of the plot (not shown), and thus it does not appear to be fractal structure. Appropriately chosen, arbitrarily close initial conditions typically lead to different attractors.

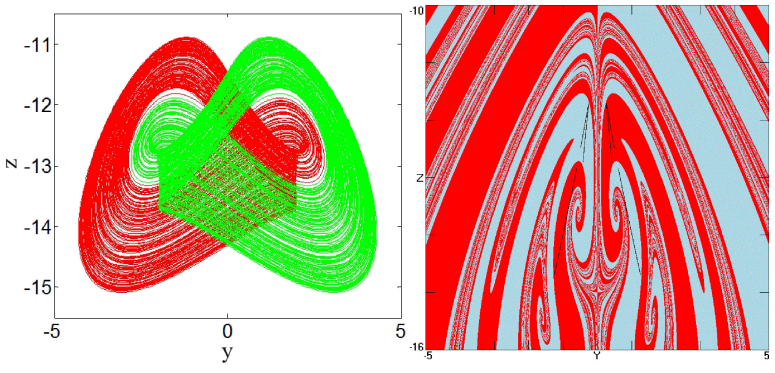

(a) (b)

Fig. 5. Coexisting symmetric pair of single-wing strange attractors when $a = 11$, $b = -9$ (a) Phase portrait in the y-z plane (red and green with symmetric initial conditions $(x_0, y_0, z_0) = 0, \pm 1, 0$ (b) Cross section for $x = 0$ of the basins of attraction.

DOI: 10.1587/elex.12.20141116
Received November 27, 2014
Accepted January 20, 2015
Publicized February 3, 2015
Copyedited February 25, 2015

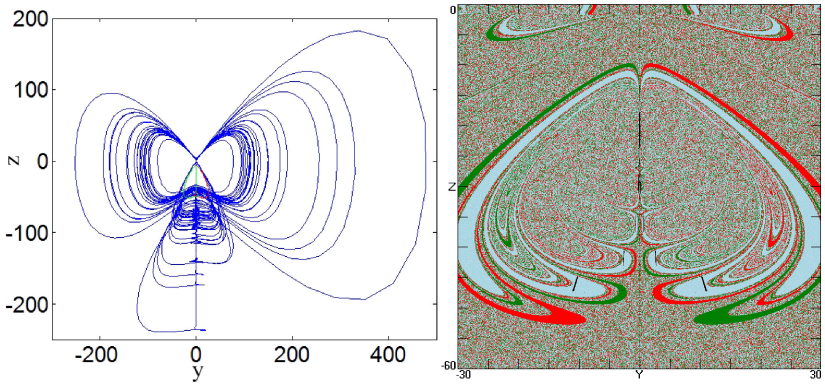

(a) (b)

Fig. 6. Coexisting symmetric pair of single-wing strange attractors when $a = 16.5$, $b = 10$ (a) Phase portrait of in the y-z plane (blue for initial conditions $(x_0, y_0, z_0) = 1, 0, 1$ red and green for symmetric initial conditions $(x_0, y_0, z_0) = \pm 1, \pm 2.5, 1$ (b) Cross section for $x = 0$ of the basins of attraction.

5 Hidden amplitude parameter and its application in a chaotic circuit

5.1 Hidden amplitude parameter in the coefficient of one quadratic term

The chaotic system with a specific wing structure attractor arises from a system with four quadratic terms, three linear terms, and one constant term. If the parameter m varies, all the equilibria will change correspondingly. The first two coordinates (x and y) of all equilibrium points will scale according to $1/\sqrt{m}$ without any change in the third coordinate (z). This special coordinate change of the equilibrium points will not influence the eigenvalues because the characteristic equation is independent of m. This leads to the important result that parameter m changes the amplitude of x and y, while the Lyapunov exponent spectrum remains constant. Thus m is a hidden amplitude parameter in this system, and it only adjusts the amplitude of the variables generated and will not lead to any bifurcations [21]. The proof follows.

Let $A = km$, $u = x/\sqrt{k}$, $v = y/\sqrt{k}$, $w = z(k > 0)$, so that the system becomes

$$\begin{cases} \dot{u} = au + v + vw, \\ \dot{v} = -uw + vw, \\ \dot{w} = -w - Auv + b, \end{cases} \tag{6}$$

which has the same form as Eq. (1). Thus the parameter m controls the amplitude of variables x and y according to $1/\sqrt{m}$. When parameter m changes by a factor of k, the variables x and y will decrease by $1/\sqrt{k}$ while the amplitude of z remains unchanged. Furthermore, the Lyapunov exponent spectrum remains unchanged.

5.2 Four-wing attractor circuit based on the hidden amplitude parameter

Here a new amplitude-adjustable four-wing chaotic circuit is designed based on this special hidden amplitude parameter. Considering the saturation property of the analog multipliers and the operational amplifiers, usually we reduce the state

DOI: 10.1587/elex.12.20141116
Received November 27, 2014
Accepted January 20, 2015
Publicized February 3, 2015
Copyedited February 25, 2015

variables by a linear transformation to avoid saturation. In this case, well known regular chaotic design procedures before designing the chaotic circuit are applied. For example, let $u = x$, $v = y/2$, and $w = z$ such that the scaled equations are given by

$$\begin{cases} \dot{u} = au + 2v + 2vw, \\ \dot{v} = -\dfrac{1}{2}uw + vw, \\ \dot{w} = -w - 2muv + b, \end{cases} \tag{7}$$

According to the above equations, we can design a normal analog circuit and output the chaotic signal for comparison with numerical solutions of the equations. However, according to the analysis in Fig. 1, the ranges of variables x and z (in volts) satisfy the requirement of not saturating the analog multipliers and operational amplifiers, while the variable y is out of the range of the hardware. So, here we construct the circuit in Fig. 7 depending on the initial equation (1), by applying a potentiometer $R7$ to realize the hidden amplitude parameter m to change the range of the variables x and y. The circuit equations in terms of the circuit parameters have the form

$$\begin{cases} \dot{x} = \dfrac{1}{R_1C_1}x + \dfrac{1}{R_2C_1}y + \dfrac{1}{R_3C_1}yz, \\ \dot{y} = -\dfrac{1}{R_4C_1}xz + \dfrac{1}{R_5C_2}yz, \\ \dot{z} = -\dfrac{1}{R_6C_3}z - \dfrac{1}{R_7C_3}xy + \dfrac{V_3}{R_8C_3} \end{cases} \tag{8}$$

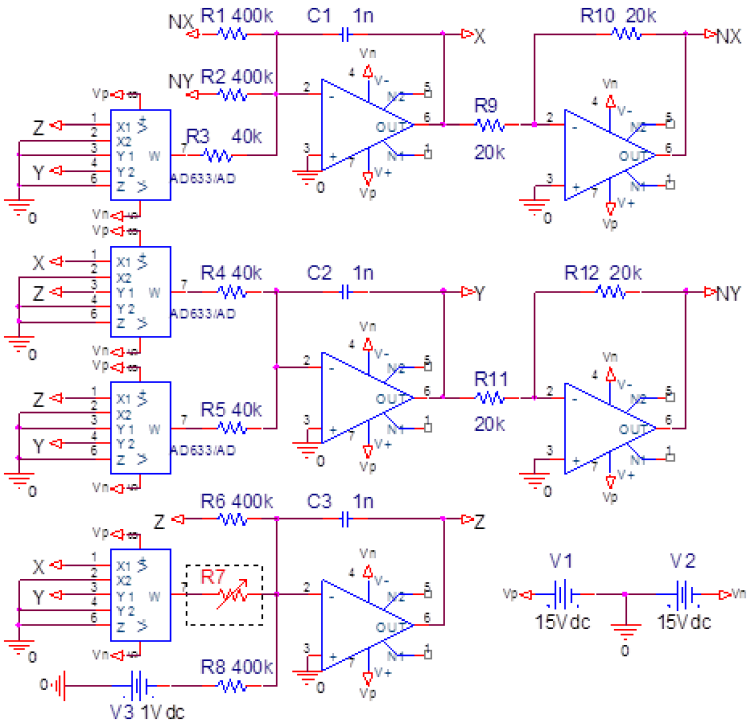

Fig. 7. Four-wing attractor circuit with amplitude parameter for amplitude adjustment

DOI: 10.1587/elex.12.20141116
Received November 27, 2014
Accepted January 20, 2015
Publicized February 3, 2015
Copyedited February 25, 2015

The circuit consists of three channels to realize the integration, addition, and subtraction of the state variables x, y, and z, respectively. The operational amplifier TL081/TI and its peripheral circuit can realize the addition, inversion and integration, and the analog multiplier AD633/AD can realize the nonlinear product operation. The state variables x, y, and z in Eq. (1) correspond to the state voltages of the three channels, respectively. When the system parameters are $a = b = m = 1$, the circuit elements have the values $R1 = R2 = R6 = R8 = 400\,\mathrm{k\Omega}$, $R3 = R4 = R5 = R7 = 40\,\mathrm{k\Omega}$, $R9 = R10 = R11 = R12 = 20\,\mathrm{k\Omega}$, and $V3 = 1\,\mathrm{V}$. To obtain a stable phase portrait in the oscilloscope, we select the capacitors $C1 = C2 = C3 = 1\,\mathrm{nF}$, which only increases the oscillation frequency of the circuit. Note that the dimension of the products in Eq. (8) does not correspond with the rest of the equation, which is because there is an implied voltage factor coming from the analog multiplier used in the circuit. We set the potentiometer $R7$ small enough to keep the amplitude of variables x and y within the limit of the hardware.

For the sake of comparison, we examine the size and shape of the attractors produced by the circuit as shown in the oscilloscope traces in Fig. 8 with the solutions of Eq. (1) in the x-y and x-z planes shown in Fig. 1. It is observed that the range of the variables x, y, and z are $[-10, 10]$, $[-20, 20]$, and $[-11, 9]$, respectively.

To decrease the range of variables x, and y, the only needed step is to change the value of potentiometer $R7$ gradually. For example, make the value of potentiometer $R7$ a quarter of the original, i.e. $R7 = 10\,\mathrm{k\Omega}$. The attractors in the x-y, x-z plane as shown in Fig. 8 are half the size of those in Fig. 1 as expected. Circuit experiment outputs show good agreement with the numerical analysis and demonstrate that the parameter m is a hidden amplitude parameter, and correspondingly the potentiometer $R7$ can control the amplitude of signals x and y, while the signal z remains in the same range as shown in Fig. 8, oscilloscope traces of system (1), at $m = 4(2\,\mathrm{V/Div})$.

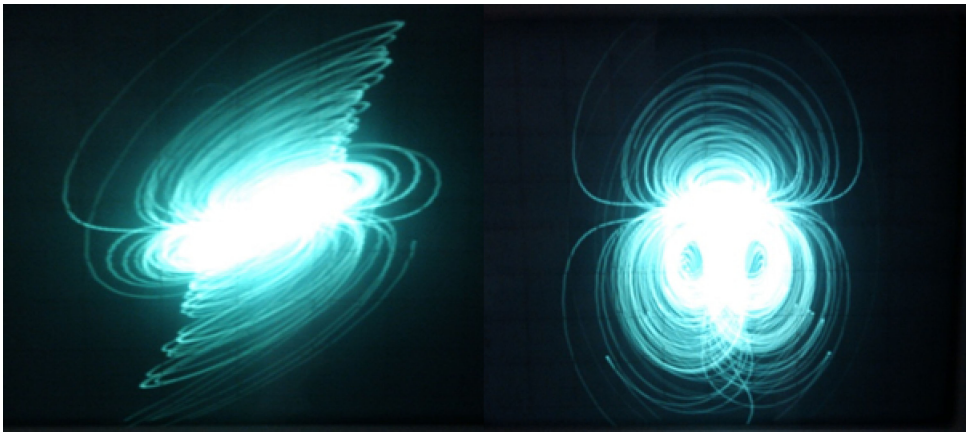

(a) (b)

Fig. 8. (a) Attractor in the x-y plane, (b) x-z plane.

DOI: 10.1587/elex.12.20141116
Received November 27, 2014
Accepted January 20, 2015
Publicized February 3, 2015
Copyedited February 25, 2015

6 Conclusions

A new four-wing attractor is constructed and analyzed. This four-wing chaotic system possesses four quadratic terms and three real equilibrium points. A distinguishing property of the system is that there are diverse routes to the wing attractor through different bistabilities. The route can be from two existing stable points to a butterfly directly, or from a symmetric limit cycle to a four-wing attractor that degrades to a butterfly, or from a coexisting symmetric pair of limit cycles to two coexisting single-wing attractors, which then form a double-wing butterfly that develops a four-wing structure. The chaos with different numbers of wings occupies most regions of parameter space. There are Arnold tongues of limit cycles stretching into the chaotic region, which shows that limit cycles are embedded in the chaotic region. Furthermore, the system has one coefficient of a quadratic term that is a hidden parameter and that controls the amplitude of two of the state variables while the system remains chaotic. A chaotic circuit is designed and constructed without linear transformation for selecting proper values of the resistors. By controlling the value of a potentiometer, the range of two signals generated by the circuit can be smoothly controlled, and the scale of the four-wing attractor is changed correspondingly. Such a four-wing attractor not only contributes an additional example of the rarely-found four-wing chaotic systems, but it is also potentially useful in chaos applications.

Acknowledgements

This work was supported by the Jiangsu Overseas Research and Training Program for University Prominent Young and Middle-aged Teachers and Presidents, the 4th 333 High-level Personnel Training Project (Su Talent [2011] No. 15) of Jiangsu Province, the National Science Foundation for Postdoctoral General Program and Special Founding Program of People's Republic of China (Grant No. 2011M500838 and Grant No. 2012T50456) and Postdoctoral Research Foundation of Jiangsu Province (Grant No. 1002004C).

DOI: 10.1587/elex.12.20141116
Received November 27, 2014
Accepted January 20, 2015
Publicized February 3, 2015
Copyedited February 25, 2015